HYDROLOGICAL PROCESSES
Hydrol. Process. **21**, 3420–3430 (2007)
Published online 24 July 2007 in Wiley InterScience
(www.interscience.wiley.com) DOI: 10.1002/hyp.6556

Incorporating variable source area hydrology into a curve-number-based watershed model

Elliot M. Schneiderman,[1]* Tammo S. Steenhuis,[2] Dominique J. Thongs,[1] Zachary M. Easton,[2] Mark S. Zion,[1] Andrew L. Neal,[2] Guillermo F. Mendoza[1] and M. Todd Walter[2]

[1] *New York City Department of Environmental Protection, 71 Smith Avenue, Kingston, NY 12401, USA*
[2] *Department of Biological and Environmental Engineering, Cornell University, Ithaca, NY 14853, USA*

Abstract:

Many water quality models use some form of the curve number (CN) equation developed by the Soil Conservation Service (SCS; U.S. Depart of Agriculture) to predict storm runoff from watersheds based on an infiltration-excess response to rainfall. However, in humid, well-vegetated areas with shallow soils, such as in the northeastern USA, the predominant runoff generating mechanism is saturation-excess on variable source areas (VSAs). We reconceptualized the SCS–CN equation for VSAs, and incorporated it into the General Watershed Loading Function (GWLF) model. The new version of GWLF, named the Variable Source Loading Function (VSLF) model, simulates the watershed runoff response to rainfall using the standard SCS–CN equation, but spatially distributes the runoff response according to a soil wetness index. We spatially validated VSLF runoff predictions and compared VSLF to GWLF for a subwatershed of the New York City Water Supply System. The spatial distribution of runoff from VSLF is more physically realistic than the estimates from GWLF. This has important consequences for water quality modeling, and for the use of models to evaluate and guide watershed management, because correctly predicting the coincidence of runoff generation and pollutant sources is critical to simulating non-point source (NPS) pollution transported by runoff. Copyright © 2007 John Wiley & Sons, Ltd.

KEY WORDS curve number; variable source area hydrology; runoff; watershed modelling; General Watershed Loading Function; non-point source pollution

Received 11 July 2005; Accepted 6 July 2006

INTRODUCTION

Watershed models that simulate streamflow and pollutant loads are important tools for managing water resources. These models typically simulate streamflow components, baseflow and storm runoff, from different land areas and then associate pollutant concentrations with the flow components to derive pollutant loads to streams. Storm runoff is the primary transport mechanism for many pollutants that accumulate on or near the land surface. Accurate simulation of pollutant loads from different land areas therefore depends as much on realistic predictions of runoff source area locations as on accurate predictions of storm runoff volumes from the source areas.

The locations of runoff production in a watershed depend on the mechanism by which runoff is generated. Infiltration-excess runoff, also called Hortonian flow (e.g. Horton 1933, 1940), occurs when rainfall intensity exceeds the rate at which water can infiltrate the soil. Soil infiltration rates are controlled by soil characteristics, vegetation and land use practices that affect the infiltration characteristics of the soil surface. In contrast, saturation-excess runoff occurs when rain (or snowmelt) encounters soils that are nearly or fully saturated due to a perched water table that forms when the infiltration front reaches a zone of low transmission (USDA-SCS, 1972). The locations of areas generating saturation-excess runoff, typically called variable source areas (VSAs), depend on topographic position in the landscape and soil transmissivity. Variable source areas expand and contract in size as water tables rise and fall, respectively. Since the factors that control soil infiltration rates differ from the factors that control VSAs, models that assume infiltration-excess as the primary runoff-producing mechanism will depict the locations of runoff source areas differently than models that assume saturation-excess.

In humid, well-vegetated areas with shallow soils, such as the northeastern USA, infiltration-excess does not always explain observed storm runoff patterns. For shallow soils characterized by highly permeable topsoil underlain by a dense subsoil or shallow water table, infiltration capacities are generally higher than rainfall intensity, and storm runoff is usually generated by saturation-excess on VSAs (Dunne and Leopold, 1978; Beven, 2001; Srinivasan *et al*., 2002; Needleman *et al*., 2004). Walter *et al*. (2003) found that rainfall intensities in the Catskill Mountains, NY, rarely exceeded infiltration rates, concluding that infiltration-excess is not a dominant runoff generating mechanism in these watersheds.

The Generalized Watershed Loading Function (GWLF) model (Haith and Shoemaker 1987, Schneiderman *et al*., 2002) uses the U.S. Department of Agriculture (USDA)

* Correspondence to: Elliot M. Schneiderman, New York City Department of Environmental Protection, 71 Smith Avenue, Kingston, NY 12401, USA. E-mail: eschneiderman@dep.nyc.gov

Copyright © 2007 John Wiley & Sons, Ltd.

Soil Conservation Service (SCS, now NRCS) runoff-curve-number (CN) method (USDA-SCS, 1972) to estimate storm runoff for different land uses or hydrological response units (HRUs). The GWLF model, like many current water quality models, uses the SCS–CN runoff equation in a way that implicitly assumes that infiltration-excess is the runoff mechanism. In short, each HRU in a watershed is defined by land use and a hydrological soil group classification via a 'CN value' that determines runoff response. Curve number values for different land use and hydrological soil group combinations are provided in tables compiled by USDA (e.g. USDA-SCS, 1972, 1986). The hydrological soil groups used to classify HRUs are based on infiltration characteristics of soils (e.g. USDA-NRCS, 2003) and thus clearly assume infiltration-excess as the primary runoff-producing mechanism (e.g. Walter and Shaw, 2005).

Here, we describe a new version of GWLF termed the Variable Source Loading Function (VSLF) model that simulates the aerial distribution of saturation-excess runoff within the watershed. The VSLF model simulates runoff volumes for the entire watershed using the SCS–CN method, but spatially distributes the runoff response according to a soil wetness index as opposed to a combination of land use and hydrological soil group as with the GWLF model. We review the SCS–CN method and the theory behind the application of the SCS–CN equation to VSAs, validate the spatial predictions made by VSLF, and compare model results between GWLF and VSLF for a watershed in the Catskill Mountains of New York State to demonstrate differences between the two approaches.

REVIEW OF THE SCS–CN METHOD

The SCS–CN method estimates total watershed runoff depth Q (mm) for a storm by the SCS runoff equation (USDA-SCS, 1972):

$$Q = \frac{(P_e)^2}{(P_e + S_e)} \tag{1}$$

where P_e (mm) is the depth of effective rainfall after runoff begins and S_e (mm) is the depth of effective available storage (mm), i.e. the spatially averaged available volume of retention in the watershed when runoff begins. We use the term effective and the subscript 'e' to identify parameter values that refer to the period after runoff starts. Although S_e in Equation (1) is typically written simply as S, this term is clearly defined for when runoff begins as opposed to when rainfall begins (USDA-SCS, 1972); thus we refer to it as S_e.

At the beginning of a storm event, an initial abstraction, I_a (mm), of rainfall is retained by the watershed prior to the beginning of runoff generation. Effective rainfall, P_e, and storage, S_e, are thus (USDA-SCS, 1972):

$$P_e = P - I_a \tag{2a}$$

$$S_e = S - I_a \tag{2b}$$

where P (mm) is the total rainfall for the storm event and S (mm) is the available storage at the onset of rainfall. In the traditional SCS–CN method, I_a is estimated as an empirically derived fraction of available storage:

$$I_a = 0{\cdot}2\ S_e \tag{3}$$

Effective available storage, S_e, depends on the moisture status of the watershed and can vary between some maximum $S_{e,max}$ (mm) when the watershed is dry, e.g. during the summer, and a minimum $S_{e,min}$ (mm) when the watershed is wet, usually during the early spring. The $S_{e,max}$ and $S_{e,min}$ limits have been estimated to vary around an average watershed moisture condition with corresponding $S_{e,avg}$ (mm) based on empirical analysis of rainfall-runoff data for experimental watersheds (USDA-SCS, 1972; Chow *et al*., 1988):

$$S_{e,max} = 2{\cdot}381\ S_{e,avg} \tag{4}$$

$$S_{e,min} = 0{\cdot}4348\ S_{e,avg} \tag{5}$$

$S_{e,avg}$ is determined via table-derived CN values for average watershed moisture conditions (CN_{II}) and a standard relationship between S_e and CN_{II}.

$$S_{e,avg} = 254\left(\frac{100}{CN_{II} - 1}\right) \tag{6}$$

However, for most water quality models, $S_{e,avg}$ (mm) is ultimately a calibration parameter that is only loosely constrained by the USDA-CN tables. Values for CN_{II} and $S_{e,avg}$ can be derived directly from baseflow-separated streamflow data when such data are available (USDA-NRCS, 1997; NYC DEP, 2006).

In the original SCS–CN method, S_e varies depending on antecedent moisture or precipitation conditions of the watershed (USDA-SCS, 1972). For VSA watersheds, a preferred method varies S_e directly with soil moisture content. We use a parsimonious method adapted from the USDA soil-plant-atmosphere-water (SPAW) model (Saxton *et al*. 1974). The value of S_e is set to $S_{e,min}$ when unsaturated zone soil water is at or exceeds field capacity, and is set to $S_{e,max}$ when soil water is less than or equal to a fixed fraction of field capacity (a parameter termed *spaw cn coeff* in VSLF), which is set to 0·6 in the SPAW model but can be calibrated in VSLF. The value for S_e is derived by linear interpolation when soil water is between $S_{e,min}$ and $S_{e,max}$ thresholds.

SCS–CN EQUATION APPLIED TO VSA THEORY

The SCS–CN equation, Equation (1), constitutes an empirical runoff–rainfall relationship. It is therefore independent of the underlying runoff generation mechanism, i.e. infiltration-excess or saturation-excess. In fact, the originator of Equation (1), Victor Mockus (Rallison 1980), specifically noted that S_e is either 'controlled by the rate of infiltration at the soil surface or by the

Copyright © 2007 John Wiley & Sons, Ltd.

DOI: 10.1002/hyp

rate of transmission in the soil profile or by the water-storage capacity of the profile, whichever is the limiting factor' (USDA-SCS, 1972). Interestingly, in later years he reportedly said 'saturation overland flow was the most likely runoff mechanism to be simulated by the method...' (Ponce, 1996).

Steenhuis *et al*. (1995) showed that Equation (1) could be interpreted in terms of a saturation-excess process. Assuming that all rain falling on unsaturated soil infiltrates and that all rain falling on areas that are saturated (to the surface or to a near-surface preferential flow zone) becomes runoff, then the rate of runoff generation will be proportional to the fraction of the watershed that is effectively saturated, A_f, which can then be written as:

$$A_f = \frac{\Delta Q}{\Delta P_e} \tag{7}$$

where ΔQ is incremental saturation-excess runoff or, more precisely, the equivalent depth of excess rainfall generated during a time period over the whole watershed area, and ΔP_e is the incremental depth of precipitation during the same time period. We define saturation-excess runoff Q in Equation (7) to include both overland flow where soil is saturated to the surface and rapid subsurface flow due to a perched water table intersecting an upper soil layer where preferential flow (i.e. unimpeded subsurface lateral flow through macropores) exists. If Q includes runoff generated by other mechanisms (e.g. infiltration excess runoff) then A_f may be overestimated. In what follows Q is exclusively saturation-excess runoff.

By writing the SCS Runoff Equation (1) in differential form and differentiating with respect to P_e, the fractional contributing area for a storm can be written as:

$$A_f = 1 - \frac{S_e^2}{(P_e + S_e)^2} \tag{8}$$

According to Equation (8) runoff occurs only on areas that have a local effective available storage σ_e (mm) less than P_e. Therefore by substituting σ_e for P_e in Equation (8) we have a relationship for the percent of the watershed area, A_s, which has a local effective soil water storage less than or equal to σ_e for a given overall watershed storage of S_e:

$$A_s = 1 - \frac{S_e^2}{(\sigma_e + S_e)^2} \tag{9}$$

Solving for σ_e gives the maximum effective (local) soil moisture storage within any particular fraction A_s of the overall watershed area, for a given overall watershed storage of S_e:

$$\sigma_e = S_e \left(\sqrt{\frac{1}{(1 - A_s)}} - 1 \right) \tag{10}$$

or, expressed in terms of local storage, σ (mm), when rainfall begins (as opposed to when runoff begins):

$$\sigma = S_e \left(\sqrt{\frac{1}{(1 - A_s)}} - 1 \right) + I_a \tag{11}$$

Equation (11) is illustrated conceptually in Figure 1. For a given storm event with precipitation P, the location of the watershed that saturates first ($A_s = 0$) has local storage σ equal to the initial abstraction I_a, and runoff from this location will be $P - I_a$. Successively drier locations retain more precipitation and produce less runoff according to the moisture–area relationship of Equation (11). The driest location that saturates defines the runoff contributing area (A_f) for a particular storm of precipitation P. The reader is reminded that both S_e and I_a are watershed-scale properties that are spatially invariant.

As average effective soil moisture (S_e) changes through the year, the moisture–area relationship will shift accordingly as per Equation (10). However, once runoff begins for any given storm, the effective local moisture storage, σ_e, divided by the effective average moisture storage, S_e, assumes a characteristic moisture–area relationship according to Equation (10) that is invariant from storm to storm (Figure 2).

Runoff q (mm) at a point location in the watershed can now also be expressed for the saturated area simply as:

$$q = P_e - \sigma_e \text{ for } P_e > \sigma_e \tag{12}$$

and for the unsaturated portion of the watershed:

$$q = 0 \text{ for } P_e \leq \sigma_e \tag{13}$$

The total runoff Q of the watershed can be expressed as the integral of q over A_f.

$$Q = \int_0^{A_f} q(\mathrm{d}A_s) \tag{14}$$

Transforming GWLF into VSLF

The GWLF model calculates runoff by applying Equation (1) separately for individual HRUs, which are distinguished by infiltration characteristics of soils and land use. The VSLF model simulates runoff from

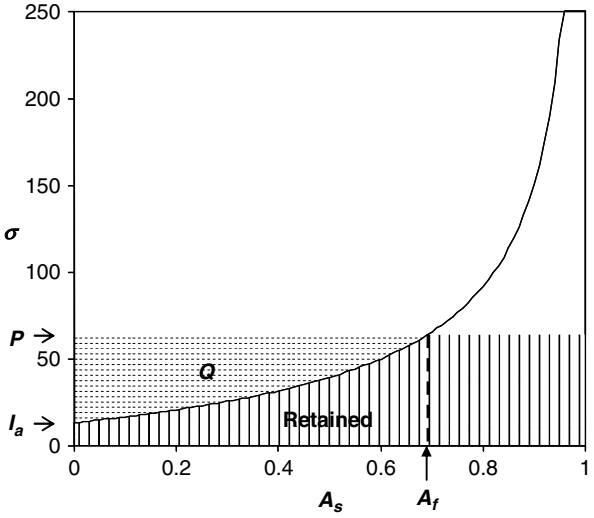

Figure 1. Relationship of available local moisture storage, σ, to the fraction of watershed area contributing runoff (A_s)

Copyright © 2007 John Wiley & Sons, Ltd.

DOI: 10.1002/hyp

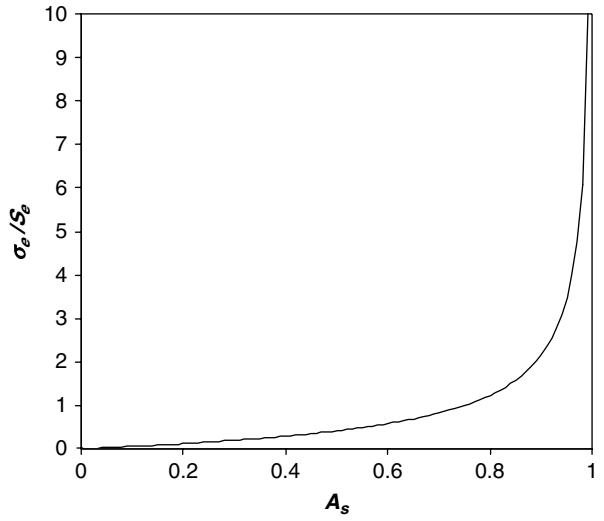

Figure 2. Relationship of effective local moisture storage, σ_e, normalized to effective average moisture storage S_e, to the fraction of watershed area contributing runoff (A_s)

HRUs dominated by impervious surfaces with the same infiltration-excess approach used in GWLF. The remaining watershed area, consisting of pervious surfaces, is treated according to the VSA CN theory developed.

In VSLF, determination of runoff from HRUs is based on a soil wetness index that classifies each unit area of a watershed according to its relative propensity for becoming saturated and producing saturation-excess storm runoff. Here we propose using the soil topographic index from TOPMODEL (Beven and Kirkby, 1979) to define the distribution of wetness indices, although VSLF does not require any specific index. A soil topographic index map of a watershed is generated by dividing the watershed into a grid of cells and calculating the index for each cell by:

$$\lambda = \ln\left(\frac{a}{T\tan\beta}\right) \tag{15}$$

where a is the upslope contributing area for the cell per unit of contour line (m), $\tan\beta$ is the topographic slope of the cell and T is the transmissivity at saturation of the uppermost layer of soil (m^2 day^{-1})—calculated from soil survey data as the product of soil depth and saturated hydraulic conductivity. This formulation neglects the impact of land use, a simplification based on the logic that, in general, there is no need for a separate water balance for each land use when saturation excess runoff is the dominant process. This assumption may cause some errors in the summer period for some land-cover types when evapotranspiration is significant, but is generally not believed to be troublesome.

The wetness index is used to qualitatively rank areas or HRUs in the watershed in terms of their overall probability of runoff. The number and/or size of the index classes depend upon the application of the user. As an example, we chose to divide the watershed into ten equal-area classes according to the wetness index, i.e. class 1 as the wettest 10% of the watershed, class 2 as the next wettest 10%, etc. The effective soil water storage within each area is determined by integrating Equation (10):

$$\sigma_{e,i} = \int_{A_{s,i}}^{A_{s,i+1}} \sigma_e \cdot d\overline{A}_s = \frac{2S_e(\sqrt{1-A_{s,i}} - \sqrt{1-A_{s,i+1}})}{(A_{s,i+1} - A_{s,i})} - S_e \tag{16}$$

where each wetness class area is bounded on one side by the fraction of the watershed that is wetter, $A_{s,i}$, i.e., the part of the watershed that has lower local moisture storage, and on the other side by the fraction of the watershed that is dryer, $A_{s,i+1}$, i.e., has greater local moisture storage. A wetness index class defined in this way may coincide with multiple land uses. Runoff depth within an index class in VSLF will be the same irrespective of land use, but nutrient concentrations are assigned to land uses independent of wetness class. Wetness index classes are thus subdivided by land use to define HRUs with unique combinations of wetness class and land use. Nutrient loads from each wetness-class–land-use HRU are tracked separately in VSLF, but otherwise are estimated as in GWLF.

In the original GWLF, runoff is calculated for each soil- and land-use-defined HRU using Equation (1). In VSLF, when precipitation occurs the contributing area fraction, A_f, is first calculated with Equation (8). Runoff is then calculated for each wetness class with Equations (12) and (13), where σ_e is determined by Equation (16). For the entire watershed, runoff depth Q is the aerially weighted sum of runoff depths q_i for all discrete contributing areas:

$$Q = \sum_{i=1}^{n} q_i(A_{s,i+1} - A_{s,i}) \tag{17}$$

The total runoff depth, Q, calculated by this equation is the same as that calculated by the SCS runoff Equation (1). The main difference between the VSLF and GWLF approaches to utilizing the SCS runoff equation is that runoff is explicitly attributable to source areas according to a wetness index distribution (e.g. Equation 15), rather than by land use and soil infiltration properties as in original GWLF. Soil properties that control saturation-excess runoff generation (saturated conductivity, soil depth) affect runoff distribution in VSLF since they are included in the wetness index.

VSLF VALIDATION

Both the integrated and distributed VSLF predictions were tested to assess its applicability to temperate, northeastern USA watersheds. Three different tests were performed: (1) we compared predicted and observed basin-scale runoff; (2) we compared the locations of VSLF predicted saturated areas to those predicted by a more rigorous physically based model, Soil Moisture Distribution and Routing (SMDR;e.g. Frankenberger *et al.*, 1999); and

Copyright © 2007 John Wiley & Sons, Ltd.

DOI: 10.1002/hyp

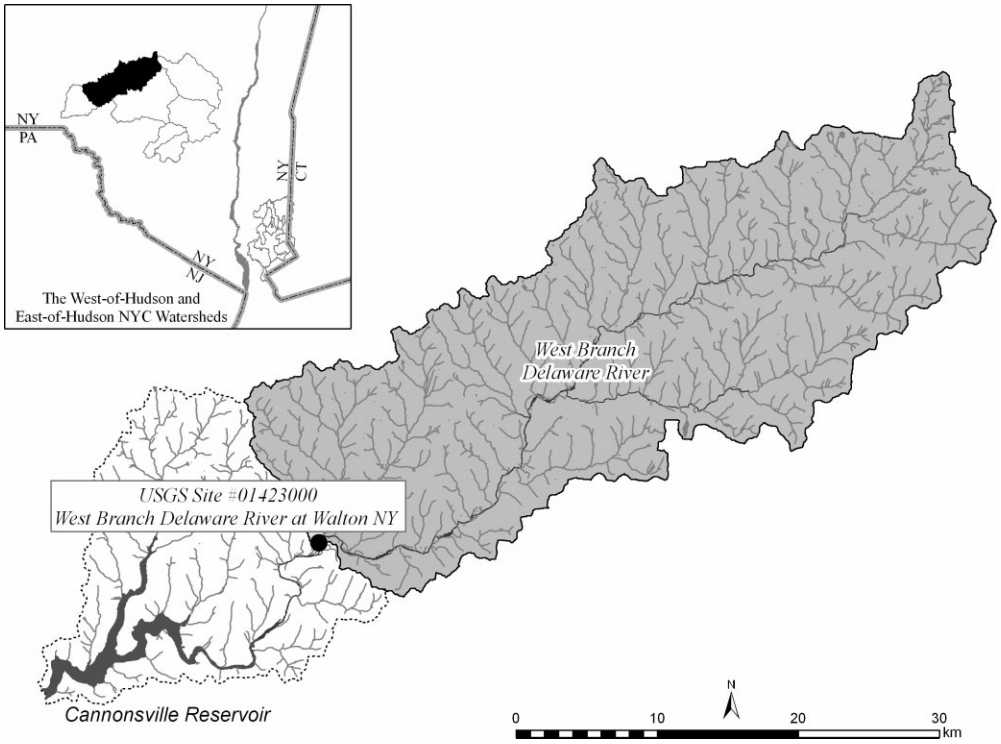

Figure 3. Location Map of the Cannonsville watershed

(3) we compared predicted and field-measured soil moisture over several transects.

These tests were performed within the Cannonsville Reservoir watershed located in the Catskill Mountain region of New York State. The Cannonsville is one of the reservoirs that supply water to New York City. It has a watershed area of 1180 km^2 and is predominately forested or agricultural land with moderate to steep hillslopes and mostly shallow soils overlying glacial till or bedrock (Schneiderman *et al*., 2002). The Cannonsville watershed upstream of the U.S. Geological Survey gauging station at West Branch Delaware River (WBDR) at Walton was used for test (1) and a small sub-basin was used for (2) and (3) (Figure 3).

For VSLF application, a wetness index map for the watershed of interest was created with ten equal-area index classes. A soil topographic index map at a 30 m grid cell resolution was made using Equation (15). The '*a*' values for Equation (15) were determined using a multidirectional flow path algorithm (Thongs and Wood, 1993). Soil depths and saturated conductivity values, required to calculate T (Equation 15), were obtained from U.S. Department of Agriculture Soil Survey Geographic (SSURGO) data. The soil topographic index map data were then aggregated to create a map of ten equal-area index classes, the wettest class being the 10% of the watershed with the highest topographic index values (i.e. corresponding to the wettest 10%), the next wettest class being the 10–20% range of next highest index values, and so on. The wetness index map was then intersected with a land use map, based on 1992 LANDSAT data, to derive areas for each wetness-index–land-use HRU.

Test 1

The VSLF model was applied to the Cannonsville watershed upstream of the WBDR at Walton U.S. geological Survey gauging station. A previous study (NYC DEP, 2006) developed and applied a methodology for calibrating the watershed $S_{e,avg}$ in GWLF against observed runoff estimates from baseflow-separated daily stream hydrograph data. The model was calibrated for 1992–1999 and a leave-one-out cross validation *(loocv)* time series (McCuen, 2005) that is independent of the calibration was developed for comparison with 1992–1999 data. Figure 4a shows the VSLF simulated event runoff (*loocv* time series) plotted against observed runoff losses at WBDR at Walton. Event runoff is defined as the direct runoff component of the baseflow-separated daily hydrograph, summed over a period that lasts from the first day of streamflow hydrograph rise until the beginning of the next event. The VSLF simulations of watershed runoff volumes for this period agree well with observed runoff data at the watershed outlet. Nash–Sutcliff efficiency (Nash and Sutcliffe, 1970) (E) was $E = 0{\cdot}86$. No systematic bias was evident in the results, with predicted versus observed data evenly scattered around the 1 : 1 line (Figure 4B).

Test 2

Figure 5 shows the spatial probability of saturated areas using VSLF and SMDR for a small sub-watershed. Probability of saturation was defined as the ratio of the 'number of days for which a location (or wetness class for VSLF) is saturated' to the 'total number of days simulated' (e.g. Walter *et al*., 2000, 2001). The VSLF

Copyright © 2007 John Wiley & Sons, Ltd.

DOI: 10.1002/hyp

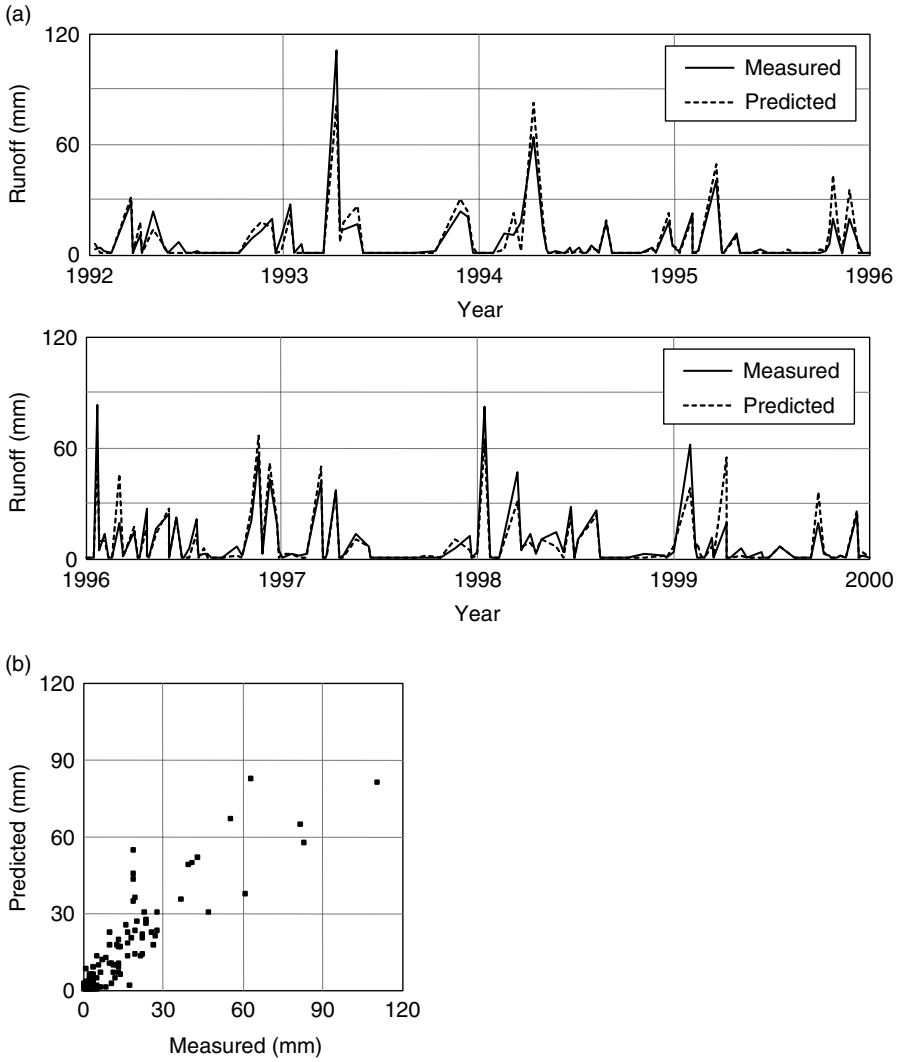

Figure 4. (A) Observed and VSLF-simulated event runoff (mm) from the Cannonsville watershed, and (B) scatterplot of observed versus predicted event runoff for 1992–1999. Observed event runoff estimated by baseflow separation of daily streamflow hydrograph. Nash–Sutcliffe efficiency was 0·86

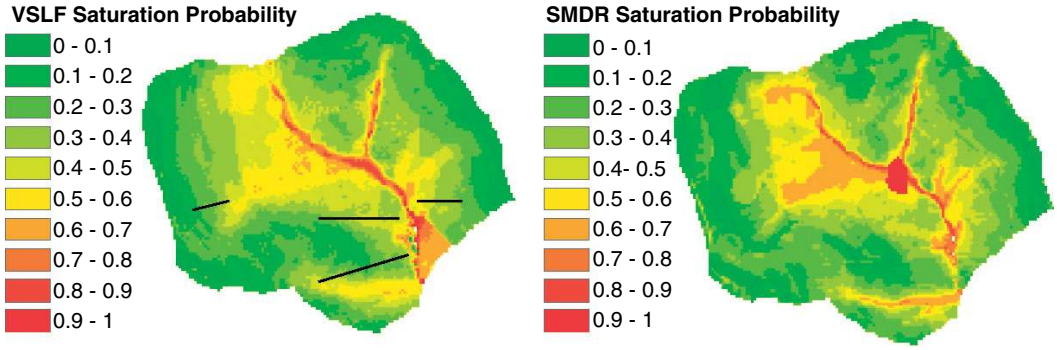

Figure 5. Probability of saturation for runoff-event predictions for a Cannonsville subwatershed using VSLF model and the Soil Moisture Distribution and Routing (SMDR) model. Soil moisture sampling transects used in Figure 6 are shown on the VSLF map

results showed similar patterns of predicted saturation as SMDR (Figure 5), which has been extensively and successfully tested in this watershed (e.g. Frankenberger *et al*., 1999; Mehta *et al*., 2004; Gerard-Marchant *et al*., 2005). It is perhaps not surprising that these two models agree so strongly since both SMDR and topographic index are strongly driven by topography. Thus, both show higher probability of saturation in the downslope areas where slopes flatten and where there is a large upslope contributing area. In both models the areas of low probability of saturation coincide with the upslope areas. There are a few differences between the distributions of saturated areas predicted by the two models (Figure 5). The VSLF model shows continuity in the distribution

Copyright © 2007 John Wiley & Sons, Ltd.

DOI: 10.1002/hyp

of saturated areas in the landscape, whereas SMDR, due to the process based computation, better predicts discontinuous saturated areas. In general, the standard error between predicted saturated area using VSLF and SMDR varied by <5%; a small fraction (<10%) had larger differences, e.g. the pond in the middle of the watershed could have been better predicted in VSLF with a few modifications.

Test 3

We used observed saturation degree data from Frankenberger *et al.* (1999) and Gérard-Marchant *et al.* (2005); the transect locations are shown in Figure 5. For each transect location the predicted saturation degree, *sd,* was calculated from the estimated moisture deficit (i.e. available local storage σ, Equation 11) and soil pore volume, V_f (mm), for that location:

$$sd = 1 - \sigma/V_f \tag{18}$$

Figure 6 shows examples of the simulated and observed saturation degree for three transects and two dates (6 May 1994 and 8 June 2001). The two lines showing the simulated results in Figure 6 represent the saturation degree when rainfall starts (dashed line, Equation 11) and when runoff is initiated (solid line, Equation 10). On both dates and all three transects, the simulated saturation degree show good agreement with the measured data. Most of the observed values fall between the simulated saturation degree estimates (Figure 6). Since variability in field soils is high, especially over 10 × 10 m grids, we have shown the sampling error (or variability) associated with each of the measured points as a shaded band (Gérard-Marchant *et al.*, 2005). For every sampling point, at least one of the predicted upper and lower saturation degrees lies within the band representing error estimates of the observed data. Thus, the observed and simulated values differ by similar or smaller magnitudes than the error or variability seen in the field.

Figure 7 shows the grouped comparison of the saturation degree from five transects and three dates. Since multiple observed points along the transect fall within a single index class, the mean of the observed saturation degree for each index class was used in the comparison. The horizontal error bars show the standard error of the range of observed values for each mean, and allow comparison of the inherent variability of soil moisture levels between transects. Overall, the saturation degree was well predicted by the model, with coefficient of determination $r^2 = 0{\cdot}76$ and $E = 0{\cdot}70$. The outlier in Figure 7 is from a late October sample when the model predicted drier conditions than observed due to underestimation of autumn precipitation for the subwatershed where the transects are located. This outlier strongly influences the regression, skewing the intercept term. Removing this point results in a slope = 1·08, and the r^2 increases to 0·79, and $E = 0{\cdot}76$. The VSLF predicted saturation degree accuracy is comparable to that predicted by fully distributed, process-based models such as SMDR.

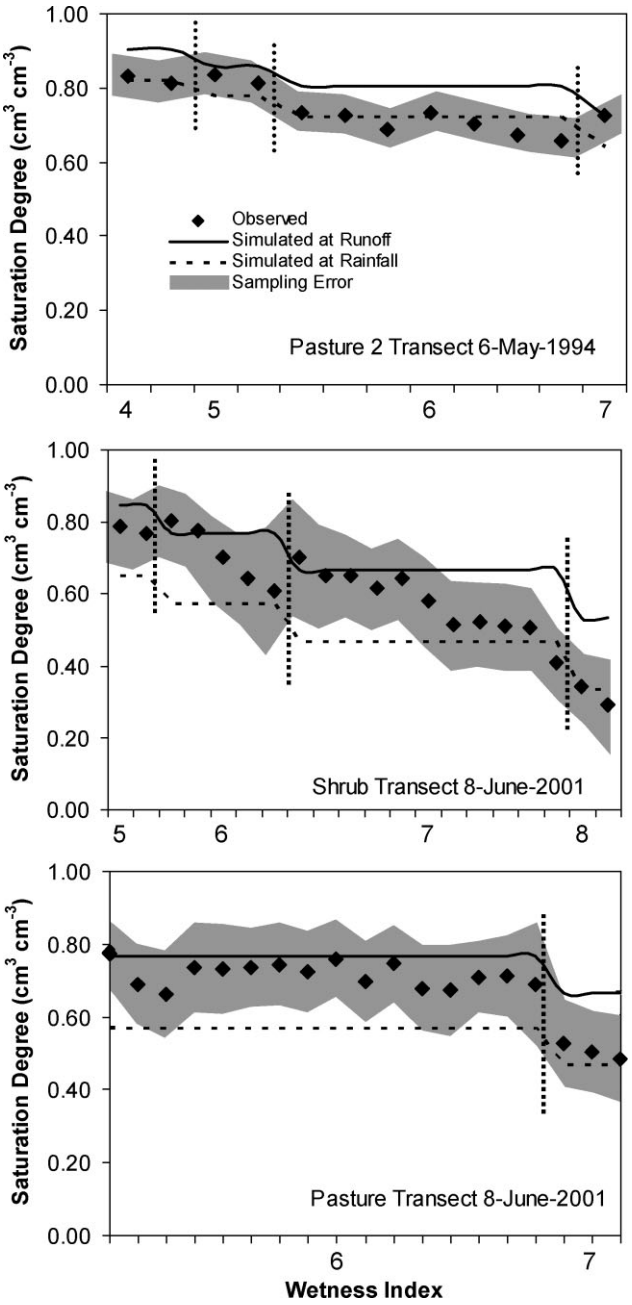

Figure 6. Observed and simulated soil moisture levels at the initiation of rainfall (long dashed line) and runoff (solid line) from three transects in the watershed. Grey area represents observed sampling error. Short vertical dashed line represents a transition between wetness index classes based on the topographic index

SPATIAL DISTRIBUTION OF RUNOFF IN VSLF VERSUS GWLF

We applied both GWLF and VSLF models to the WBDR at Walton watershed, upstream of the Cannonsville Reservoir, to compare spatial patterns of runoff as predicted by the two models. The GWLF model was applied using the SPAW method for varying S_e with soil moisture and the calibrated parameters from the VSLF model application (test 1 above), to be consistent with the VSLF application to WBDR at Walton. Runoff at the watershed outlet predicted with the two models is very similar (Figure 8).

Copyright © 2007 John Wiley & Sons, Ltd.

DOI: 10.1002/hyp

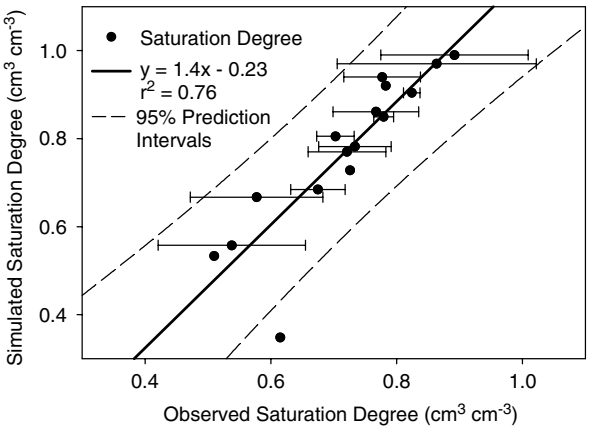

Figure 7. Scatter plot of observed and the Variable Source Loading Function (VSLF) model simulated soil moisture levels from five dates and three transects in both the growing and dormant seasons in the R-Farm subwatershed. Since numerous observed values fall within the same index class along the transect, the mean observed value was regressed against each individual index class. Horizontal bars represent the standard error of the observed saturation degree for each index class

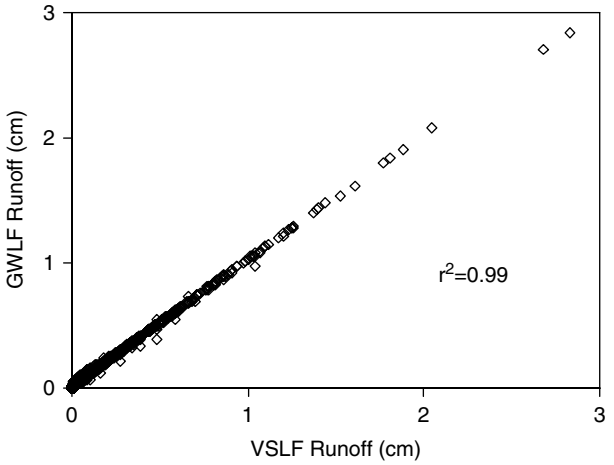

Figure 8. Scatter plot of the Generalized Watershed Loading Function (GWLF) model versus the Variable Source Loading Function (VSLF) model simulated event runoff for the Cannonsville watershed

Slight differences are due to the fact that VSLF calculates runoff for the total pervious area of the watershed using a single parameter ($S_{e,avg}$), whereas GWLF calculates runoff separately for each individual land use. The spatial distribution of runoff predicted by VSLF and GWLF is, as expected, markedly different. The GWLF runoff predictions are controlled by the spatial pattern of land use and, to a lesser degree, soils, whereas VSLF runoff predictions follow the pattern of the wetness index. Figure 9a and b depicts the land use map and wetness indices, respectively, for an example subarea of Cannonsville watershed. Figure 9c–f shows how the underlying spatial patterns in Figure 9a and b correspond to the distribution of runoff predictions. Depicted are average runoff predictions over the simulation period for a dry period of the year, July, and a wet period of the year, April. For both models, there is overall more runoff generated in April, when watershed moisture conditions are wettest, than in July. However, GWLF predicts that most of the runoff comes from cornfields and predicts all cornfields generate runoff equally (Figure 9c and e); indeed, any given land use has uniform runoff predicted from it regardless of its location in the watershed. This, of course, follows from the fact that the original GWLF model, like most water quality models, use tabulated $S_{e,avg}$ (or CN_{II}) values based on tables that correlate runoff response to land use and soil type. For example, on these tables, cornfields have one of the highest runoff responses, i.e., lowest $S_{e,avg}$ (highest CN_{II}). In contrast, the spatial pattern of runoff predicted by VSLF follows the pattern of the wetness index, with high wetness index areas generating most of the runoff; compare Figure 9b with 9d and f.

DISCUSSION

The model developed here is essentially an amalgam of VSA ideas that have been developed over the past several years. For example, wetness indices have been used to effectively predict VSAs for watersheds dominated by saturation-excess runoff (e.g. Western *et al*., 1999), and topographic indices have been used outside the TOPMODEL (Beven and Kirkby, 1979) framework to predict VSAs (e.g. Lyon *et al*., 2004; Agnew *et al*., 2006). By using a wetness index to spatially distribute runoff, the VSLF model more realistically predicts the locations of runoff production in saturation-excess dominated watersheds than the original GWLF model, which distributes runoff by land use and soil infiltration rate (Figure 9). Thus it follows that the distribution of runoff generation in VSLF agrees conceptually with the our scientific understanding of VSA hydrology (e.g. Hewlett and Hibbert, 1967; Dunne and Black, 1970; Dunne and Leopold, 1978; Frankenberger *et al*., 1999; Western *et al*., 1999, 2004; Beven, 2001; Mehta *et al*., 2004; Niedzialek and Ogden, 2004).

The application of the SCS–CN method to VSAs presented here is an extension of the ideas proposed by Steenhuis *et al*. (1995) and, especially, Lyon *et al*. (2004). Lyon *et al*. (2004) used Equation (8) to determine the fraction of the watershed contributing for a given effective precipitation and identified the specific contributing area via a topographic index, Equation (15). Lyon *et al*. (2004) assumed that after runoff started there was only one storage parameter S for the whole watershed independent of initial wetness. In the new version presented here, S is a function of overall watershed wetness, which is a conceptual improvement over the constant S approach used by Steenhuis *et al*. (1995) and Lyon *et al*. (2004). In addition, the method presented here predicts spatially variable runoff depths within a saturated area, whereas the Lyon *et al*. (2004) approach assigns a single runoff depth to the entire saturated area. Since this is an average depth, the Lyon *et al*. (2004) approach will underpredict the amount of runoff generated near streams, which may be a critical area of non-point contaminant loading in many watersheds. Some other minor differences between the Lyon *et al*. (2004) approach and the new version are that the initial abstraction used here is

Copyright © 2007 John Wiley & Sons, Ltd.

DOI: 10.1002/hyp

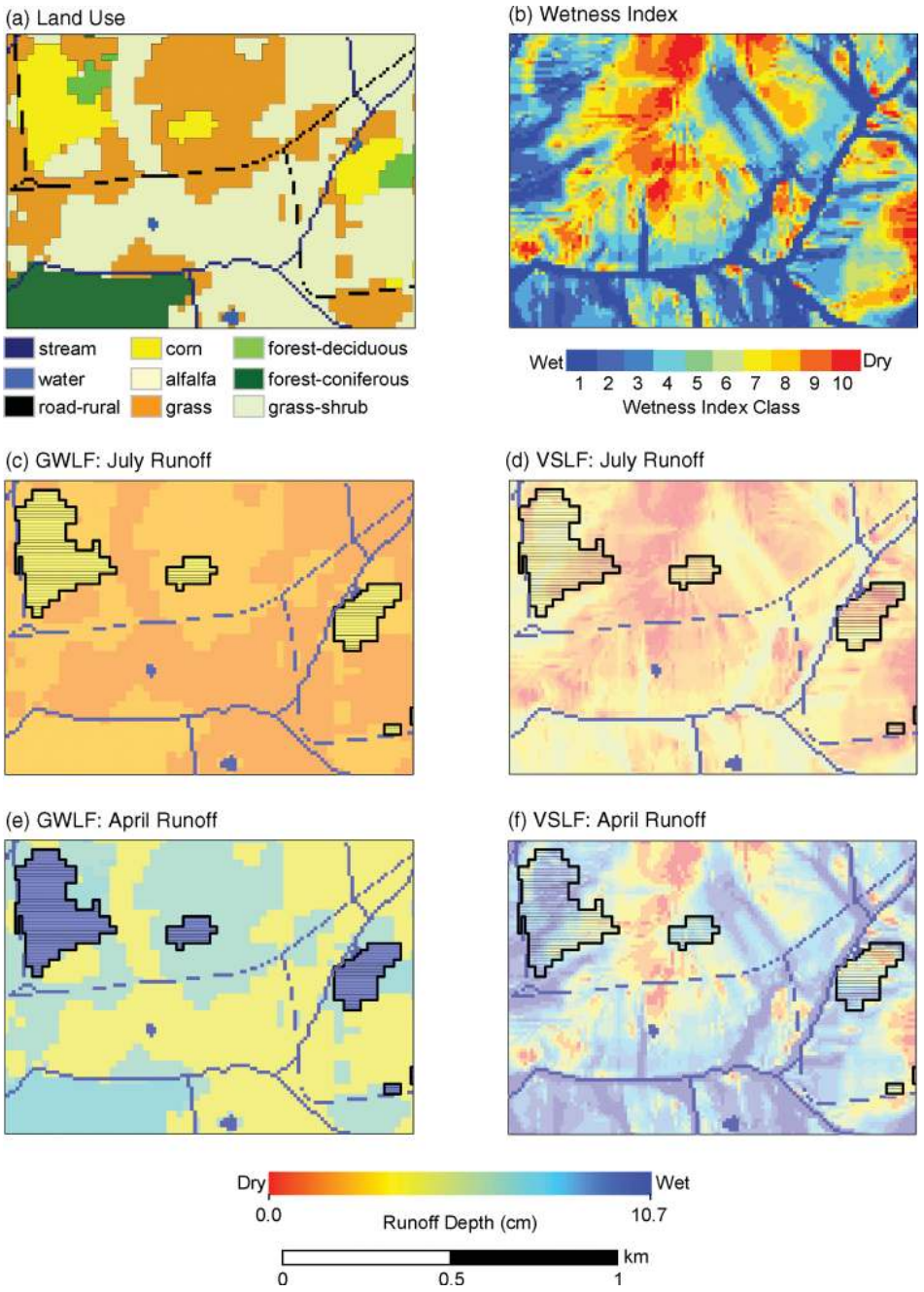

Figure 9. Maps, for an example subarea of Cannonsville watershed, of: (a) land use; (b) wetness index; (c) mean July runoff predicted by GWLF; (d) mean July runoff predicted by VSLF; (e) mean April runoff predicted by GWLF; (f) mean April runoff predicted by VSLF. Corn fields are outlined in heavy black lines

a constant fraction of the average storage whereas Lyon *et al*. (2004) used a water budget approach. In both cases I_a changes with watershed wetness so it is not obvious that one approach is more realistic than the other.

Accurate prediction of the spatial distribution of runoff production has important consequences for simulation of pollutants that are typically transported by runoff. Many water quality protection concepts have been developed based on results from models such as GWLF, which link runoff and pollutant concentrations to land use. As a result, we have sometimes focused too much attention on specific land uses and largely ignored the interaction between land management and landscape position; indeed, Garen and Moore (2005) have explicitly noted this problem for all models that use the SCS–CN method in similar ways. For example, our GWLF simulations suggest that nutrient management should be focused entirely on cornfields (Figure 9c and e). However, VSLF, which better represents the spatial hydrological patterns, indicates that control of nutrients from areas near streams might be more logical locations to focus water quality protection efforts. In this case grasslands located in high runoff producing areas constitute a potentially important land use to manage (Figure 9d and f). More importantly, VSLF provides a more complete picture of intra-watershed processes and facilitates a broader range of

Copyright © 2007 John Wiley & Sons, Ltd.

DOI: 10.1002/hyp

potentially important NPS pollution processes. It should probably be noted that the original GWLF (Haith and Shoemaker, 1987) was not designed to give this level of spatially explicit detail, and VSLF represents the way that models may be diverted over time from their original scope of purpose (e.g. Garen and Moore, 2005; Walter and Shaw, 2005).

CONCLUSIONS

The SCS–CN method for estimating runoff is used in many current non-point-source pollution models to simulate infiltration-excess runoff. These models assume that runoff generation and pollutant loading are tightly linked to land use, and other factors that directly impact soil infiltration capacity. For humid, well-vegetated watersheds, however, saturation-excess on VSAs is the predominant runoff mechanism, and runoff generation is more indicative of landscape position than land use. We describe an alternative SCS–CN-based approach to predicting runoff that is applicable to VSA watersheds and should be relatively easy to implement in existing models. We spatially validated the predictions made by the model and, as a demonstration, showed that in watersheds where saturation-excess is the dominant runoff process the new VSLF model provides a much more valid spatial distribution of runoff generation than current SCS–CN-based water quality models.

ACKNOWLEDGEMENTS

We would like to acknowledge our reviewers, one of which pointed out that that variable source areas do not have to be saturated to the surface to produce runoff. This is correct and has led us to redefine the definition of storm runoff and variable source areas. Other reviewers also made very helpful comments and due to their efforts the manuscript has improved greatly. The USDA-CSREES, USDA-NRI, and NSF-REU programs partially funded the involvement of the Soil and Water Laboratory from Cornell's Biological and Environmental Engineering Department.

REFERENCES

Agnew LJ, Lyon S, Gérard-Marchant P, *et al*. 2006. Identifying hydrologically sensitive areas: Bridging science and application. *Journal of Environmental Management* **78**: 64–76.

Beven K. 2001. *Rainfall–Runoff Modeling: The Primer*. Wiley: Chichester; 360 pp.

Beven KJ, Kirkby MJ. 1979. A physically-based, variable contributing area model of basin hydrology. *Hydrological Science Bulletin* **24**: 43–69.

Chow VT, Maidment DR, Mays LW. 1988. *Applied Hydrology*. McGraw-Hill: New York; 572 pp.

Dunne T, Black RD. 1970. Partial area contributions to storm runoff in a small New England watershed. *Water Resources Research* **6**: 1296–1311.

Dunne T, Leopold L. 1978. *Water in Environmental Planning*. W.H. Freeman: New York; 818 pp.

Frankenberger JR, Brooks ES, Walter MT, Walter MF, Steenhuis TS. 1999. A GIS-based variable source area model. *Hydrological Processes* **13**(6): 804–822.

Garen DC, Moore DS. 2005. Curve number hydrology in water quality modeling: uses, abuses, and future directions. *Journal of the American Water Resources Association* **41**(2): 377–388.

Gérard-Marchant P, Hively WD, Steenhuis TS. 2005. Distributed hydrological modeling of total dissolved phosphorus transport in an agricultural landscape, part I: distributed runoff generation. *Hydrology and Earth Systems Science Discussions* **2**: 1537–1579.

Haith DA, Shoemaker LL. 1987. Generalized Watershed Loading Functions for stream flow nutrients. *Water Resources Bulletin* **23**(3): 471–478.

Hewlett JD, Hibbert AR. 1967. Factors affecting the response of small watersheds to precipitation in humid regions. In *Forest Hydrology*, Sopper WE, Lull HW (eds). Pergamon Press: Oxford; 275–290.

Horton RE. 1933. The role of infiltration in the hydrologic cycle. *Eos (Transactions of the American Geophysical Union)* **14**: 44–460.

Horton RE. 1940. An approach toward a physical interpretation of infiltration-capacity. *Soil Science Society of America Proceedings* **5**: 399–417.

Lyon SW, Walter MT, Gerard-Marchant P, Steenhuis TS. 2004. Using a topographic index to distribute variable source area runoff predicted with the SCS curve-number equation. *Hydrological Processes* **18**(15): 2757–2771.

McCuen RH. 2005. Accuracy assessment of peak discharge models. *Journal of Hydrologic Engineering* **10**(1): 16–22.

Mehta VK, Walter MT, Brooks ES, *et al*. 2004. Evaluation and application of SMR for watershed modeling in the Catskill Mountains of New York State. *Environmental Modeling and Assessment* **9**(2): 77–89.

Nash JE, Sutcliffe JV. 1970. River flow forecasting through conceptual models, Part 1—a discussion of principles. *Journal of Hydrology* **10**: 282–290.

Needleman BA, Gburek WJ, Petersen GW, Sharpley AN, Kleinman PJA. 2004. Surface runoff along two agricultural hillslopes with contrasting soils. *Soil Science Society of America Journal* **68**: 914–923.

NYC DEP. 2006. *New York City's 2006 Watershed Protection Program Summary and Assessment, Appendix 4: Cannonsville GWLF Model Calibration and Validation*. New York City Department of Environmental Protection: Valhalla, New York.

Niedzialek JM, Ogden FL. 2004. Numerical investigation of saturated source area behavior at the small catchment scale. *Advances in Water Resources* **27**(9): 925–936.

Ponce VM. 1996. *Notes of my conversation with Vic Mockus*. http://mockus.sdsu.edu.

Rallison RE. 1980. Origin and evolution of the SCS runoff equation. *Symposium on Watershed Management*, American Society of Civil Engineers: New York, NY; 912–924.

Saxton KE, Johnson HP, Shaw RH. 1974. Modeling evaptranspiration and soil moisture. *Transactions of the American Society of Agricultural Engineers* **17**(4): 673–677.

Schneiderman EM, Pierson DC, Lounsbury DG, Zion MS. 2002. Modeling the hydrochemistry of the Cannonsville Watershed with Generalized Watershed Loading Functions (GWLF). *Journal of the American Water Resources Association* **38**(5): 1323–1347.

Srinivasan MS, Gburek WJ, Hamlett JM. 2002. Dynamics of stormflow generation—a field study in east-central Pennsylvania, USA. *Hydrological Processes* **16**(3): 649–665.

Steenhuis TS, Winchell M, Rossing J, Zollweg JA, Walter MF. 1995. SCS runoff equation revisited for variable-source runoff areas. *American Society of Civil Engineers, Journal of Irrigation and Drainage Engineering* **121**: 234–238.

Thongs DJ, Wood E. 1993. Comparison of topographic soil indexes derived from large and small scale digital elevation models for different topographic regions. Presented at *American Geophysical Union Spring Meeting*, Baltimore, MD.

USDA-NRCS. 1997. *National Engineering Handbook*, Part 630 Hydrology, Section 4, Chapter 5. Natural Resources Conservation Service, U.S. Department of Agriculture.

USDA-NRCS. 2003. *National Soil Survey Handbook, title 430-VI.* Natural Resources Conservation Service, U.S. Department of Agriculture. http://soils.usda.gov/technical/handbook/.

USDA-SCS. 1972. *National Engineering Handbook*, Part 630 Hydrology, Section 4, Chapter 10. Natural Resources Conservation Service, U.S. Department of Agriculture.

USDA-SCS. 1986. *Urban Hydrology for Small Watersheds*, Technical Release No. 55. Soil Conservation Service, U.S. Department of Agriculture. U.S. Government Printing Office: Washington, DC.

Copyright © 2007 John Wiley & Sons, Ltd.

DOI: 10.1002/hyp

Walter MT, Shaw SB. 2005. Discussion: 'Curve number hydrology in water quality modeling: Uses, abuses, and future directions' by Garen and Moore. *Journal of American Water Resources Association* **41**(6): 1491–1492.

Walter MT, Walter MF, Brooks ES, Steenhuis TS, Boll J, Weiler KR. 2000. Hydrologically sensitive areas: variable source area hydrology implications for water quality risk assessment. *Journal of Soil and Water Conservation* **3**: 277–284.

Walter MT, Brooks ES, Walter MF, Steenhuis TS, Scott CA, Boll J. 2001. Evaluation of soluble phosphorus transport from manure-applied fields under various spreading strategies. *Journal of Soil and Water Conservation* **56**(4): 329–336.

Walter MT, Mehta K, Marrone AM, *et al*. 2003. A simple estimation of the prevalence of Hortonian flow in New York City's watersheds. *American Society of Civil Engineers, Journal of Hydrologic Engineering* **8**(4): 214–218.

Western AW, Grayson RB, Bloschl G, Willgoose GR, McMahon TA. 1999. Observed spatial organization of soil moisture and its relation to terrain indices. *Water Resources Research* **35**(3): 797–810.

Western AW, Zhou SL, Grayson RB, McMahon TA, Bloschl G, Wilson DJ. 2004. Spatial correlation of soil moisture in small catchments and its relationship to dominant spatial hydrological processes. *Journal of Hydrology* **286**(1–4): 113–134.

Copyright © 2007 John Wiley & Sons, Ltd.

DOI: 10.1002/hyp